Chemical Science

ROYAL SOCIETY OF CHEMISTRY

EDGE ARTICLE

View Article Online
View Journal | View Issue

Cite this: *Chem. Sci.*, 2026, **17**, 1039

All publication charges for this article have been paid for by the Royal Society of Chemistry

Received 6th August 2025
Accepted 2nd November 2025

DOI: 10.1039/d5sc05956a

rsc.li/chemical-science

Electricity-driven site-selective deuteration of pharmaceuticals

Minling Zhong,†[a] Feihu Wang,†[a] Guanqun Han,†[a] Shuai Yuan,[b] Guodong Li,[a] De-en Jiang *[b] and Yujie Sun *[a]

Precision deuteration at metabolically vulnerable sites of pharmaceuticals can enhance drug stability and therapeutic efficacy, yet existing methods often suffer from poor selectivity and inefficiency. Here, we report an electricity-driven bromine-mediated deuteration strategy that enables late-stage site-selective deuteration of pharmaceuticals using D_2O as the deuterium source. This approach involves a two-step process: (i) bromination of labile C–H bonds using Br_2, followed by (ii) electricity-driven deuterodebromination using a palladium membrane reactor. This design leverages *in situ* Br_2 generation at the anode and selective deuterium permeation through the palladium membrane cathode, thereby significantly improving atom economy and energy efficiency. Our method achieves nearly complete conversion and >90% deuterium incorporation for a range of aryl, heteroaryl, benzylic, and unactivated alkyl bromides, including ten marketed drug molecules. Furthermore, gram-scale synthesis of D-clonidine demonstrates the scalability of this approach. By integrating high selectivity, broad substrate scope, and operational efficiency, this method offers a practical solution for deuterated drug synthesis, with potential applications in pharmaceutical development and metabolic stabilization.

Introduction

Isotopic substitution has long been recognized as a powerful tool in physical and medicinal chemistry, owing to the kinetic isotope effect that influences bond dissociation energies and reaction rates. Deuteration, the selective replacement of hydrogen with its heavier isotope deuterium, has emerged as a crucial strategy in drug development and metabolism studies.[1,2] The incorporation of deuterium can significantly alter pharmacokinetic properties by enhancing metabolic stability, reducing toxicity, and prolonging drug half-life.[3–5] Over the past few years, several deuterated pharmaceuticals have gained regulatory approval, such as deutetrabenazine (Austedo®),[6] deuremidevir (VV116),[7] and d_1-(*R*)-pioglitazone (PXL065)[8] shown in Fig. 1a. With at least 15 additional deuterated drug candidates currently in clinical trials,[9] the pharmaceutical industry continues to explore deuteration as a means to develop safer and more efficacious therapeutics. To facilitate the synthesis of deuterated drugs, various deuteration strategies have been developed. A widely used approach involves deuterated building blocks (see representative examples in Fig. 1b), which introduce deuterium into molecules at early synthetic stages.[10] While offering high isotopic enrichment, these methods typically rely on expensive and limited deuterated precursors and require multistep synthetic sequences, leading to high overall cost and operational complexity. Alternatively, direct hydrogen–deuterium exchange (H/D exchange) methods provide a more straightforward route to introduce deuterium into existing molecules. Although such methods can be effective, they often require D_2 gas, elevated temperatures, or stoichiometric additives, and may suffer from low site selectivity, incomplete labeling, or over-deuteration of complex scaffolds. With the advancement of transition-metal catalysis, H/D exchange reactions catalyzed by Pd, Ir, Ru, Rh, and Fe have become well-established in synthetic chemistry.[11–17] Nevertheless, most homogeneous catalytic systems depend on costly metals and sophisticated ligands and may raise environmental and sustainability concerns, thereby limiting their broader applicability.[18]

To address these challenges, numerous catalytic deuteration strategies have been developed, enabling deuterium incorporation into complex molecules under milder conditions and with greater atom efficiency (Fig. 1c).[19] For instance, enzymatic deuteration primarily relies on alcohol dehydrogenases and amine oxidases to achieve regioselective deuterium incorporation from D_2O.[20,21] Photocatalytic deuteration utilizes visible-light-activated catalysts to enable efficient H/D or X/D exchange,[22–30] while electrocatalytic deuteration offers another modular and energy-efficient strategy.[31–35] Although substantial progress has been achieved in recent years, the field continues

[a]*Department of Chemistry, University of Cincinnati, Cincinnati, OH 45221, USA. E-mail: yujie.sun@uc.edu*

[b]*Department of Chemical & Biomolecular Engineering, Vanderbilt University, Nashville, TN 37235, USA. E-mail: de-en.jiang@vanderbilt*

† Equally contributed.

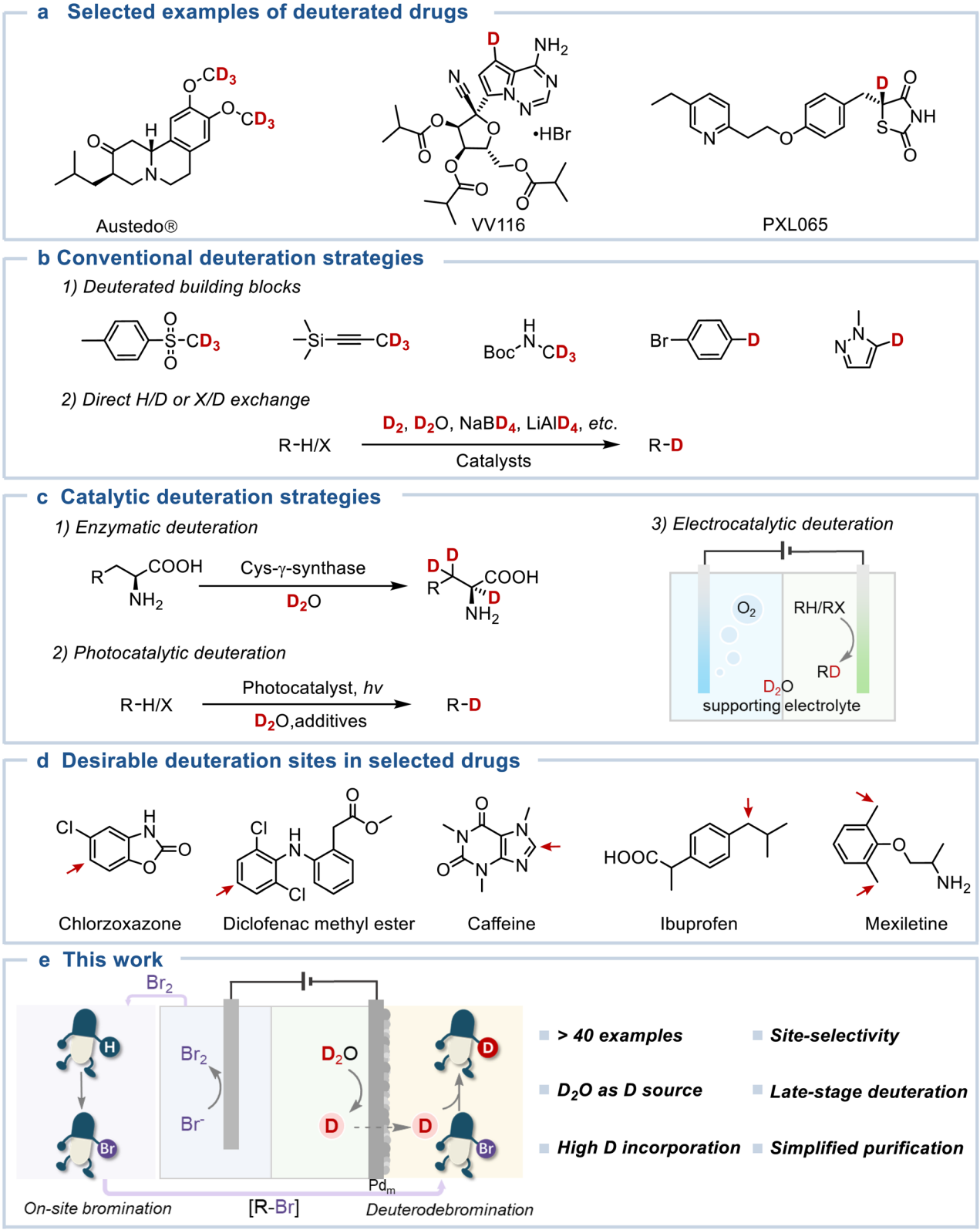

Fig. 1 Development of deuteration strategies. (a) Representative deuterated pharmaceuticals. (b) Conventional deuteration strategies. (c) Various catalytic deuteration strategies. (d) Desirable deuteration sites in selected drugs. (e) Our strategy of electricity-driven site-selective deuteration.

to face intrinsic challenges related to catalyst cost, product purification, undesired side processes, and insufficient compatibility with pharmaceutically relevant functional groups. Thus, the development of a broadly applicable and efficient protocol for late-stage deuteration, particularly at metabolically sensitive sites within drug molecules, remains an outstanding goal in synthetic and medicinal chemistry.

Precision deuteration at metabolically soft positions is critical because many pharmaceuticals undergo rapid clearance *via* cytochrome P450-mediated hydroxylation.[36,37] The strategic replacement of metabolically weak C–H bonds with C–D bonds can significantly modulate the rate of oxidative metabolism through the kinetic isotope effect, ultimately improving drug stability, prolonging systemic exposure, and reducing the required dosage and frequency of administration.[38] Moreover, precise and selective deuterium incorporation can fine-tune the pharmacokinetic and pharmacodynamic profiles of drug candidates without altering their fundamental biological targets, providing a powerful means for optimizing clinical performance. Despite these benefits, existing deuteration methods remain inadequate for achieving site-specific isotopic modification in structurally complex drug molecules. Conventional approaches either require pre-installed deuterium at the target site, which limits flexibility in modifying existing drugs, or lead to non-selective over-deuteration, potentially altering molecular properties and introducing unknown pharmaceutical risks. In fact, the desirable deuteration sites of quite a few drug molecules have been determined with representative examples shown in Fig. 1d. However, the development of a general and efficient strategy capable of achieving site-selective deuteration at metabolically relevant positions remains challenging.

Herein, we present a bromine-mediated deuteration strategy that enables precise late-stage deuteration of various drug molecules. This approach consists of a two-step process as shown in Fig. 1e: (i) bromination of metabolically labile sites in drug molecules using Br_2, followed by (ii) electricity-driven deuterodebromination in an electrochemical palladium membrane reactor (ePMR). The latter step takes advantage of the selective deuterium permeation from a D_2O-based electrolyte into a separate reaction chamber where deuterodebromination takes places.[39] Unlike conventional electrocatalysis, this spatially separated deuteration design eliminates product contamination from electrolytes, simplifying purification and improving isotopic purity. Additionally, our method leverages bromide oxidation at the anode, which reduces the required voltage input compared to conventional electrocatalytic deuteration systems usually using water oxidation as the counter reaction. Furthermore, the *in situ* generated Br_2 at the anode can be extracted to brominate additional drug molecules, further enhancing atom economy and sustainability. Beyond enabling the precise deuteration of 10 deuterated drug molecules, our approach is equally applicable in producing a variety of deuterated building blocks. Finally, gram-scale synthesis of deuterated clonidine has been successfully demonstrated, highlighting its great promise and broad utility in pharmaceutical and synthetic chemistry applications.

Results and discussion

Confirmation of hydride transfer

Conventional electrocatalytic hydrodehalogenation (*i.e.*, hydrogenolysis) typically proceeds *via* initial one-electron reduction of an organic halide, generating a carbon radical intermediate upon halide release. Subsequent proton-coupled electron transfer to this radical species leads to the formation of the hydrogenated product. A competing pathway involves radical dimerization, which can reduce the efficiency of the process. Alternatively, at highly negative potentials, direct two-electron reduction of organic halides generates carbanion intermediates, which subsequently undergo protonation to afford the hydrogenated product. However, such extreme potentials inevitably promote competitive proton reduction, leading to excessive H_2 evolution (HER) and diminished faradaic efficiency. Regardless of the mechanistic pathway, hydrodehalogenation fundamentally requires a net $2e^-/H^+$ transfer, which can be conceptually framed as a formal hydride (H^-) transfer process. This perspective aligns with emerging electrochemical strategies that leverage controlled hydrogen atom manipulation to achieve selective transformations.

The ePMR has garnered significant attention for organic hydrogenation due to the rapid diffusion of hydrogen atom through the palladium lattice.[40–43] However, previous studies predominantly focused on the hydrogenation of unsaturated substrates (*e.g.*, alkenes, alkynes, aldehydes, and nitriles) *via* hydrogen atom transfer (HAT) from the palladium membrane electrode (Pd_m). While effective for these transformations, HAT alone is insufficient for hydrodehalogenation, which requires an overall hydride transfer process. Given that hydrogen atom disproportionation has been proposed as a route to generate hydrides,[44] our initial objective was to confirm the formation and utilization of a hydride species on the hydrogenation side of Pd_m (opposite to its electrochemical interface) as illustrated in Fig. 2a. To probe this mechanism, we employed *N*-methylnicotinamide (NA^+) as a hydride acceptor, drawing inspiration from the NAD^+/NADH redox cycle. Constant-current electrolysis at -50 mA cm^{-2} was applied to the electrochemical chamber, facilitating proton/water reduction at the Pd_m surface and generating hydrogen atoms. These hydrogen atoms subsequently permeated through the membrane into a separate chamber containing 5 mM NA^+ in a phosphate buffer (pH 8) with 30% methanol (v/v). After 24 hours of electrolysis, the UV-visible absorption spectrum of the hydrogenation solution exhibited a pronounced absorption peak at 305 nm (Fig. 2b), indicative of NA^+ reduction and subsequent dearomatization. Structural confirmation *via* ^1H NMR (Fig. 2c) and mass spectrometry (Fig. 2d) revealed the formation of 1-methylpiperidine-3-carboxamide, a product consistent with hydride transfer to NA^+ followed by hydrogenation of two C=C bonds—an overall one-hydride–four-hydrogen transfer process. To further validate the hydrogen source, we replaced H_2O with D_2O in the electrochemical chamber. This modification resulted in the incorporation of five deuterium atoms into the product (Fig. 2c and d), unambiguously confirming that the hydrides (or

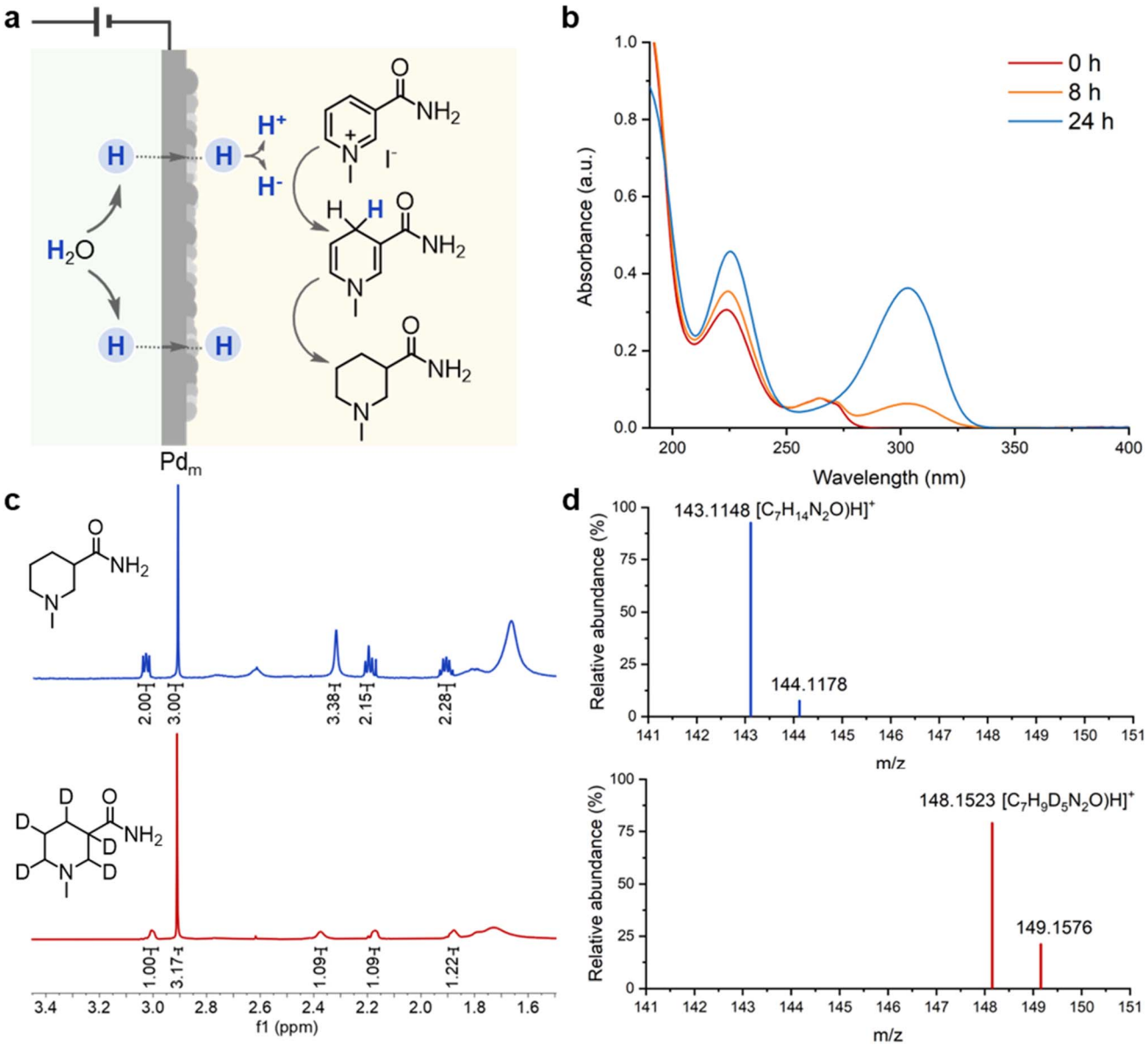

Fig. 2 Hydrogenation of *N*-methylnicotinamide (NA^+) using ePMR. (a) Proposed schematics of NA^+ hydrogenation following a one-hydride–four-hydrogen transfer mechanism. (b) UV-visible absorption spectra of the hydrogenation solution. (c) ^1H NMR spectra of the hydrogenation (top) and deuteration (bottom) solutions. (d) Mass spectroscopies of the hydrogenation (top) and deuteration (bottom) solutions.

deuterides) originate from electrochemical H_2O/D_2O reduction on the Pd_m surface. These findings demonstrate the feasibility of hydrogen/deuterium disproportionation in protic solvents using Pd_m for hydride/deuteride transfer.

Optimization of deuterodebromination

To evaluate the efficacy of the Pd_m in facilitating electrocatalytic deuterodebromination, we employed D_2O as a cost-effective deuterium source. 2-Bromoquinoline was selected as a model substrate due to the ubiquity of quinoline-based structural motifs in pharmaceuticals. Notably, the C2-position of the quinoline ring, present in the widely used antimalarial drug quinine, is metabolically susceptible to oxidation, making it a relevant target for selective deuteration.[45] We first conducted 10-hour electrolysis at -50 mA cm^{-2} with the chemical chamber containing 20 mM 2-bromoquinoline in various solvents to determine the optimal conditions for deuterium incorporation. Due to the limited solubility of 2-bromoquinoline in water, we explored methanol as a protic solvent. As summarized in Fig. 3a, methanol enabled near-complete conversion (95%) of 2-bromoquinoline, with a deuterium incorporation efficiency of 89%. In contrast, aprotic solvents resulted in significantly lower yields: 72% in tetrahydrofuran and 37% in chloroform. A parallel investigation with 4-bromotoluene under identical conditions revealed that only methanol enabled full conversion (99%) and near-quantitative deuterium incorporation (99%), whereas the other solvents were ineffective. These results

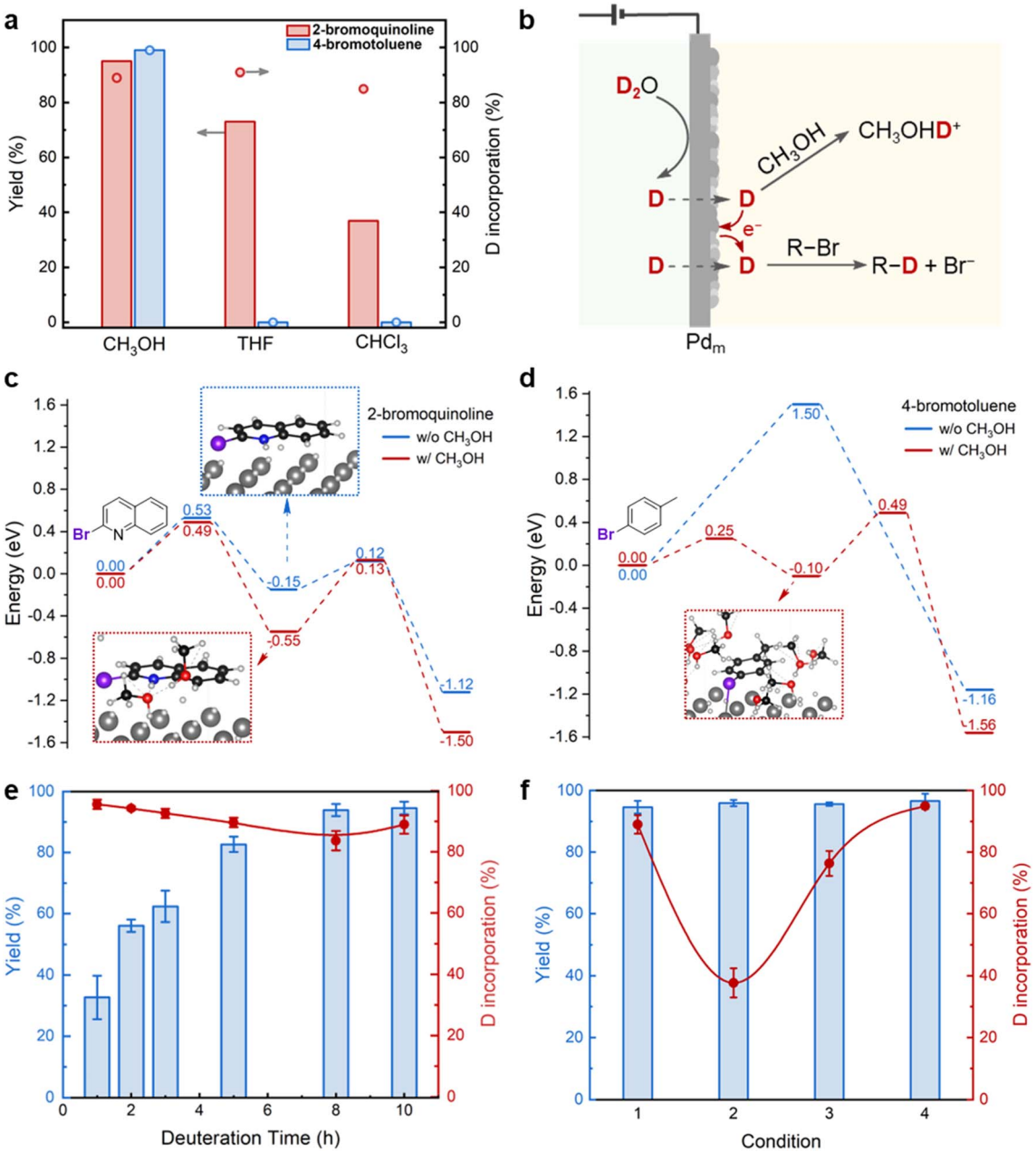

Fig. 3 Reaction development. (a) Yields and deuterium (D) incorporations after electrolysis at −50 mA cm^{-2} for 10 hours. Condition: two-compartment ePMR, Pt mesh as the anode, Pd_m as the cathode, 1.0 M $NaClO_4$ in D_2O as the electrolyte, 2-bromoquinoline or 4-bromotoluene (20 mM) in different solvents inside the deuteration chamber. (b) Proposed mechanism for the CH_3OH-assisted deuterodebromination of organic bromides using ePMR. (c and d) Calculated energy profiles of the hydrodebromination of (c) 2-bromoquinoline and (d) 4-bromotoluene on β-PdH surfaces in the absence and presence of CH_3OH. (e) Time-dependent yield and deuterium incorporation. Default condition: two-compartment ePMR, Pt mesh as the anode, Pd_m as the cathode, 1.0 M $NaClO_4$ in D_2O as the electrolyte, 2-bromoquinoline (20 mM) in CH_3OH in the deuteration chamber, −50 mA cm^{-2}. (f) Yield and deuterium incorporation of 2-bromoquinoline under different conditions. Condition 1: default condition, −50 mA cm^{-2} for 10 hours; condition 2: 10% H_2O (v/v) added to the electrolyte solution; condition 3: 10% H_2O (v/v) added to the deuteration chamber; condition 4: CD_3OD as the solvent in the deuteration chamber.

suggest that methanol plays a crucial role in promoting deuterodebromination using ePMR. To probe the reaction mechanism, 5 equivalents of 2,2,6,6-tetramethylpiperidine-1-oxyl (TEMPO) were introduced as a radical scavenger into a methanol solution of 20 mM 2-bromoquinoline in the chemical chamber. After electrolysis at −50 mA cm^{-2} for 10 h, only TEMPO-H was detected by ^1H NMR and HR-MS (Fig. S3 and S4). No TEMPO–quinoline adduct or radical dimerization products were observed, suggesting that the deuterobromination in ePMR system does not proceed through a radical pathway. As depicted in Fig. 3b, we hypothesize that methanol facilitates deuterium disproportionation on Pd_m, leading to effective

deuteride transfer to organic bromides. Additionally, in the case of 2-bromoquinoline, the nitrogen atom can be protonated, inducing the disproportionation process and enabling hydride transfer even in aprotic solvents.

To gain deeper mechanistic insights, we conducted density functional theory calculations to simulate the hydrogen-saturated Pd_m for the hydrodebromination reaction by using surface models created from the bulk β-PdH structure (see SI for details). The results presented in Fig. 3c and d strongly support our hypothesis. In the absence of methanol, protonation of the nitrogen atom in 2-bromoquinoline by an H atom on the PdH surface occurs with an energy barrier of 0.53 eV, followed by a facile hydride transfer from the PdH surface with a barrier of 0.27 eV. When methanol is present, the protonation barrier is only slightly reduced (0.49 eV), and the resulting protonated 2-bromoquinoline is further stabilized *via* hydrogen bonding, while the hydrodebromination step requires a slightly higher activation energy of 0.68 eV. A striking contrast is observed for 4-bromotoluene, where direct hydride transfer is kinetically infeasible in the absence of methanol, requiring a high activation energy of 1.50 eV. However, introduction of methanol substantially reduces the overall energy barrier, with hydride transfer becoming the rate-determining step at a reduced energy barrier of 0.59 eV—even lower than that for 2-bromoquinoline. Collectively, the above experimental and computational findings establish that, in N-heteroaromatic systems, the substrate nitrogen induces H/D atom disproportionation. By contrast, in hydrocarbon substrates, methanol acts as a critical facilitator of H/D disproportionation, thereby enabling efficient hydride/deuteride transfer using Pd_m. This mechanistic insight provides a strong foundation for realizing selective late-stage deuteration strategies in pharmaceuticals and beyond.

Given the solubility constraints of many organic bromides, methanol was chosen as the protic solvent in the deuteration chamber for all subsequent experiments unless otherwise specified. Electrolysis at -50 mA cm^{-2} using D_2O as the electrolyte solvent resulted in a steady conversion of 2-bromoquinoline (20 mM) to quinoline-2-d, reaching >95% conversion after 10 hours (Fig. 3e). The initial deuterium incorporation exceeded 95%, but a slight decrease to ~89% was observed over time, suggesting a minor source of hydrogen contamination. To systematically identify the origin of this contamination, we conducted control experiments (Fig. 3f). Introducing 10% H_2O (v/v) into the D_2O electrolyte (condition 2) significantly reduced deuterium incorporation to 37%, indicating that residual H_2O in the electrolyte chamber plays a dominant role in hydrogen contamination. In contrast, adding 10% H_2O to the deuteration chamber (condition 3) resulted in a less severe contamination, with deuterium incorporation decreasing to 76%. Notably, replacing methanol with CD_3OD (condition 4) yielded the highest deuterium incorporation (95%), further confirming that methanol in the deuteration chamber may contribute to limited H/D exchange but to a much lesser extent than electrolyte contamination. Importantly, high conversion efficiencies (>95%) were observed under all conditions, regardless of the presence of H_2O in either chamber. These results establish that adventitious H_2O in the electrolyte chamber is the primary source of hydrogen contamination, whereas methanol in the deuteration chamber exhibits only a minor influence on isotopic purity.

Substrate scope

Encouraged by the efficient deuterodebromination of 2-bromoquinoline and 4-bromotoluene *via* ePMR, we sought to evaluate the generality of our strategy across a broad range of organic bromides (Fig. 4). Aryl bromides bearing electron-donating (*e.g.*, methoxy, alkyl) and electron-withdrawing (*e.g.*, ester, amide, chlorine) groups underwent efficient deuterodebromination under standard conditions (20 mM substrate, -50 mA cm^{-2}, 10 h), yielding the corresponding deuterated arenes in high yields (**1–9**). 2-Bromoanthracene (**10**) also gave high deuterium incorporation under the standard conditions, despite its relatively low reactivity. Notably, dibromoaryl substrate **11** exhibited near-quantitative deuterium incorporation at both positions, demonstrating the strategy's efficacy for multi-site deuteration. Given the widespread presence of heteroaryl motifs in pharmaceuticals and bioactive molecules, we extended our investigation to pyridine (**12–18**), quinoline (**19**, **20**), isoquinoline (**21**), and pyrimidine (**22**) derivatives. The reaction proved highly effective in most cases, delivering excellent conversion and high deuterium incorporation, highlighting its compatibility with heteroaryl-containing systems. Benzylic bromides, which are frequently encountered in pharmaceuticals and synthetic intermediates, also exhibited high reactivity under our conditions. A diverse set of substituted benzyl bromides (**23–31**) were smoothly deuterated, yielding the desired benzylic C–D bonds with high efficiency (75–99% yield, 88–99% deuterium incorporation). Unactivated alkyl bromides, often considered challenging substrates due to their low faradaic efficiency in electrochemical deuterodehalogenation,[46] were also successfully deuterated. For instance, 1-bromo-4-phenylbutane (**32**) underwent smooth conversion, affording its deuterated product in 97% yield with 98% deuterium incorporation after 24-hour electrolysis. These results establish ePMR as a highly versatile platform for deuterodebromination, enabling site-selective deuteration across aryl, heteroaryl, benzylic, and unactivated alkyl bromides. This system was successfully applied to produce deuterated pharmaceutical building blocks, including deuterated benzoic acid (**33**),[47] *p*-toluic acid (**34**),[48] and nicotinic acids (**35–36**),[49,50] which can be employed as precursors to synthesize specifically deuterated drug molecules. The broad substrate compatibility, combined with high conversion efficiency and excellent isotopic purity, underscores the potential of this method for the synthesis of high-value deuterated building blocks—with significant implications for pharmaceuticals, agrochemicals, and materials science.

Selective deuteration of pharmaceuticals

The broad substrate compatibility of our deuterodebromination strategy suggests strong potential for late-stage deuteration of drug molecules. Many pharmaceuticals undergo *in vivo* degradation through cytochrome P450 (CYP)-mediated oxidation, necessitating strategies to minimize metabolic clearance and enhance drug stability.[36] Typically, the most labile C–H bonds,

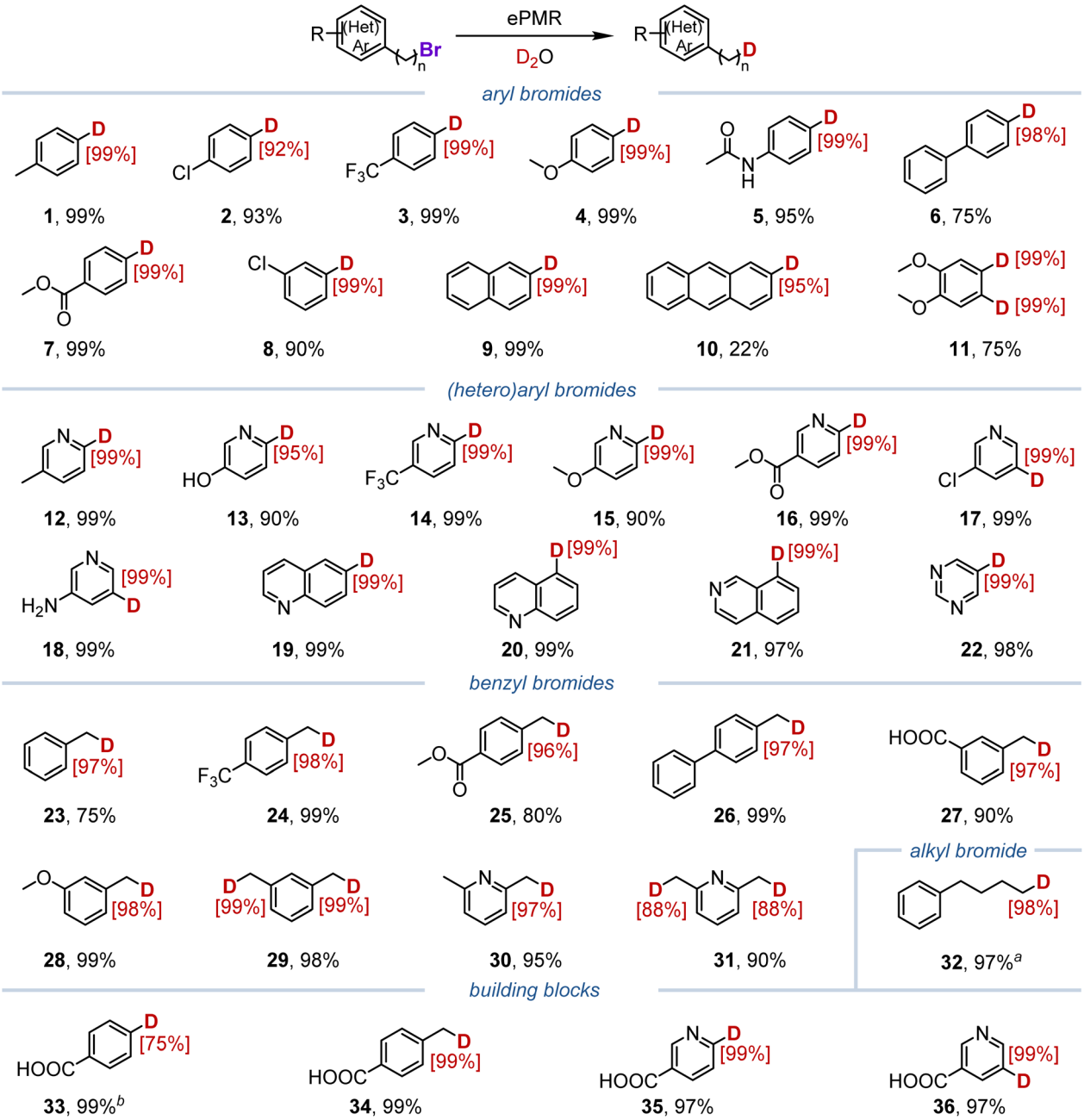

Fig. 4 Scope of electricity-driven deuterodebromination of organic bromides using ePMR. Default condition: 20 mM substrate in CH_3OH, −50 mA cm^{-2}, 10 hours. Yield and deuterium incorporation (in red brackets) were determined from ^1H NMR spectroscopy. [a] $t = 24$ h. [b] $t = 20$ h.

often termed metabolic soft sites, are the primary targets for CYP oxidation.[37] Replacing these C–H bonds with C–D bonds provides a means to slow systemic clearance, reduce dosing frequency, and enhance pharmacological efficacy.[38] Given that bromination may selectively activate these metabolically labile sites, we hypothesized that our two-step bromination–deuterodebromination approach would enable late-stage, site-selective deuteration of pharmaceuticals. To test this hypothesis, we selected ten marketed drugs whose metabolic vulnerabilities are well-documented but the specific deuteration at these sites has not been thoroughly investigated (Fig. 5).

Chlorzoxazone, a muscle relaxant and analgesic, is metabolized predominantly *via* 6-hydroxylation, a pathway linked to toxic aromatic oxirane intermediates.[51] Bromination with Br_2 in methanol (50 °C, 12 h) yielded the desired Br-chlorzoxazone (80%), which underwent smooth electrochemical deuterodebromination to afford D-chlorzoxazone with excellent yield (97%) and deuterium incorporation (97%). Similar results were observed for clonidine, an antihypertensive drug primarily metabolized *via* CYP-mediated 4-hydroxylation.[52] Treatment with 0.6 equivalents of Br_2 in methyl *tert*-butyl ether (MTBE) produced Br-clonidine (80%), which, under electrochemical deuterodebromination, furnished D-clonidine (97% yield, 95%

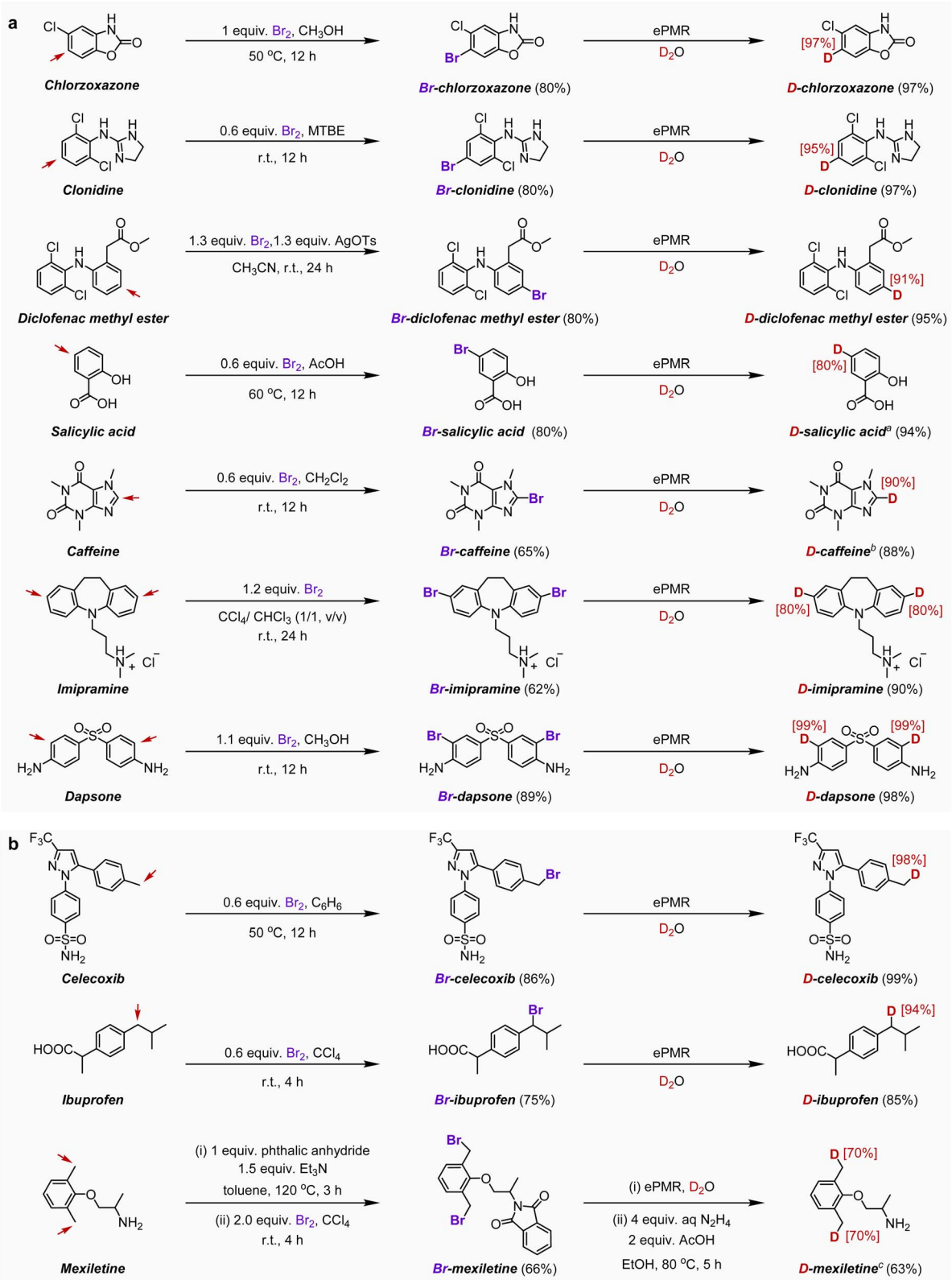

Fig. 5 Bromine-assisted selective deuteration of pharmaceuticals using ePMR. Default ePMR deuterodebromination condition: two-compartment ePMR, Pt mesh as the anode, Pd_m as the cathode, 1.0 M $NaClO_4$ in D_2O as the electrolyte, 20 mM substrate in CH_3OH in the deuteration chamber, −50 mA cm^{-2} for 10 hours. Conversion yields and deuterium incorporation ratios (in red brackets) were determined *via* ^1H NMR spectroscopy. [a] 10 mM substrate in CD_3OD in the deuteration chamber, $t = 96$ h. [b] CH_3OH/CH_2Cl_2 (v/v = 1/1) in the deuteration chamber. [c] 10 mM substrate in CH_3OH/CH_2Cl_2 (v/v = 1/1) in the deuteration chamber.

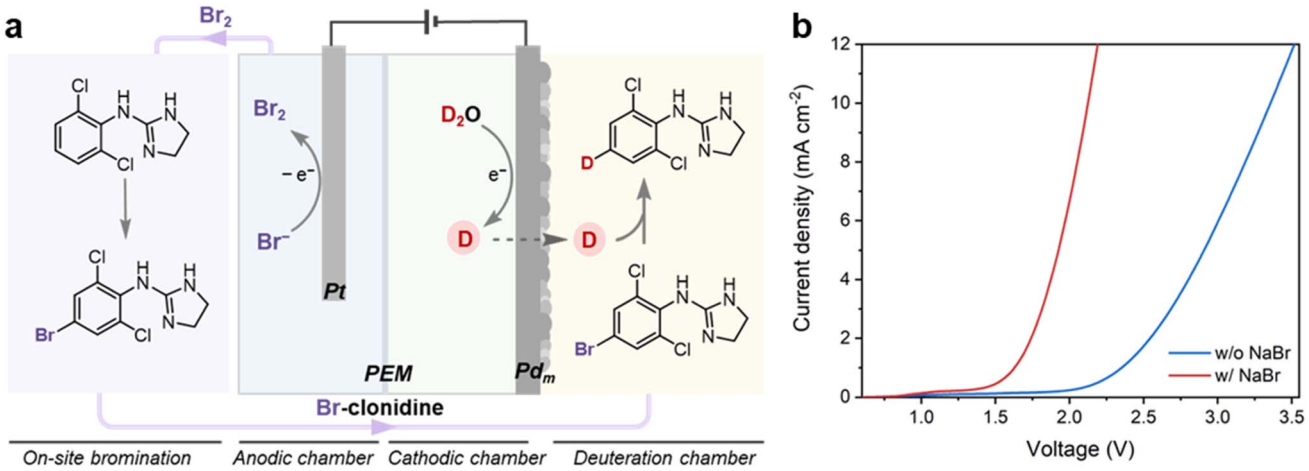

Fig. 6 Two-step bromination-deuterodebromination for the synthesis of D-clonidine. (a) Simplified scheme of ePMR coupled with on-site bromination. Pt mesh as the anode, Pd_m as the cathode; the anodic and cathodic chambers are separated by proton-exchange membrane (PEM). The electrolyte is 0.5 M D_2SO_4 in D_2O, with additional 4.0 M NaBr in the anolyte. (b) Linear sweep voltammograms collected in the absence and presence of 4.0 M NaBr in the anode chamber. Condition: two-compartment ePMR, Pt mesh as the anode, Pd_m as the cathode, 0.5 M $NaClO_4$ in H_2O as the electrolyte, scan rate = 100 mV s^{-1}.

D-incorporation). Diclofenac, a non-steroidal anti-inflammatory drug (NSAID) with a short plasma half-life, undergoes metabolism at the C5-position, forming 5-hydroxy-diclofenac as its primary phase I metabolite.[53] Bromination of diclofenac methyl ester selectively produced 5-Br-diclofenac methyl ester, which was further converted to D-diclofenac methyl ester under the default electrochemical deuterodebromination condition. Salicylic acid, a precursor to aspirin[54] and a plant hormone,[55] can also be used to treat various skin disorders.[56] Bromination with Br_2 in glacial acetic acid at 60 °C for 12 h afforded Br-salicylic acid in 80% yield. Despite the presence of phenolic hydroxyl and carboxyl groups, subsequent electrochemical deuterodebromination in CD_3OD successfully delivered D-salicylic acid with 94% yield and 80% deuterium incorporation. Caffeine, a widely consumed stimulant, is primarily metabolized *via* CYP-mediated demethylation, generating paraxanthine, which subsequently undergoes further oxidation before excretion.[57,58] To extend its pharmacokinetic half-life, our strategy selectively incorporated deuterium at the 8′-position, yielding D-caffeine (88% yield, 90% D-incorporation). For drugs containing two metabolically vulnerable positions, such as imipramine[59] and dapsone,[60] our strategy successfully enabled double deuteration at both target sites, achieving high selectivity and efficiency.

Beyond aromatic C(sp^2)–H oxidation, benzylic C(sp^3)–H hydroxylation is another prevalent metabolic pathway (Fig. 5b). For example, celecoxib undergoes benzyl hydroxylation,[61] a process that can be mitigated by deuterium substitution. Electrochemical deuterodebromination of Br-celecoxib yielded D-celecoxib with 99% yield and 98% deuterium incorporation. Similarly, ibuprofen[62] and mexiletine,[63] both metabolized at benzylic positions, underwent efficient site-selective deuteration under our optimized conditions. Collectively, these results highlight the broad utility, robustness, and adaptability of our site-selective electricity-driven deuteration strategy across diverse drug scaffolds, establishing it as a promising tool for pharmaceutical development and metabolic optimization.

Gram-scale synthesis of D-clonidine

The efficacy and scalability of our two-step bromination–deuterodebromination strategy were demonstrated in the gram-scale synthesis of deuterated clonidine (D-clonidine). As illustrated in Fig. 6a, bromide oxidation (4.0 M NaBr in electrolyte) at the anode generated Br_2 *in situ*, as evidenced by the increase of cell voltage and the characteristic color change observed in the anodic chamber (Fig. S3 and S4). The electrochemically generated Br_2 was subsequently extracted with methyl *tert*-butyl ether and used for selective bromination of clonidine at room temperature, yielding Br-clonidine in 80% yield. Simultaneously, in the deuteration chamber, Br-clonidine (0.1 M in methanol) underwent constant-current electrochemical deuterodebromination using D_2O as the deuterium source, affording D-clonidine in 97% yield with 95% deuterium incorporation (0.9 g). The final product required only methanol removal for isolation and purification, streamlining the synthesis. This strategy not only maximizes atom economy by continuously recycling bromine but also enhances energy efficiency. As shown in Fig. 6b, in the absence of NaBr, water oxidation requires a high cell voltage of 3.36 V to achieve 10 mA cm^{-2}. However, in the presence of 4.0 M NaBr, bromide oxidation enables the same current density at a significantly reduced voltage of 2.13 V, saving over 1.2 V in energy input. These results establish our electrocatalytic bromination–deuterodebromination strategy as a practical and energy-efficient approach for scalable late-stage deuteration, with direct implications for the synthesis of isotopically labeled pharmaceuticals.

Conclusion

This work presents a selective, scalable, and energy-efficient strategy for precise deuterium incorporation into diverse molecular frameworks. By integrating electricity-driven deuterodebromination with *in situ* Br_2 generation in a palladium

membrane reactor, our method enables site-selective deuteration using D_2O as the deuterium source. It enhances atom economy, energy efficiency, achieving nearly complete conversion with over 90% deuterium incorporation across aryl, heteroaryl, benzylic, and unactivated alkyl substrates while simplifying product purification. The successful gram-scale synthesis of D-clonidine further demonstrates its scalability. Its broad functional group compatibility and applicability to pharmaceuticals make it a powerful tool for metabolic stabilization and drug development. As demand for deuterated compounds grows, this method offers a practical and versatile solution for high-precision deuteration.

Author contributions

Y. S. conceived the idea and supervised the project. M. Z., F. W., G. H., and G. L. performed experimental work and data analysis. S. Y. and D. J. provided the computational support. M. Z. and Y. S. wrote the manuscript.

Conflicts of interest

The authors declare the following competing financial interest(s): Y. S. has filed a US provisional patent application no. 63/843964 (filed July 14, 2025) on the work presented in this manuscript. The remaining authors declare no other competing interests.

Data availability

Further queries about the data can be directed to the corresponding authors.

The data supporting this article have been included as part of the supplementary information (SI). Supplementary information is available. See DOI: **https://doi.org/10.1039/d5sc05956a**.

Acknowledgements

Y. S. thanks support from the US National Science Foundation (CBET-2411506) and the Petroleum Research Foundation (66635-ND3). D. J. thanks the US National Science Foundation (CHE-2245564).

References

1 J. Atzrodt, V. Derdau, W. J. Kerr and M. Reid, Deuterium-and tritium-labelled compounds: applications in the life sciences, *Angew. Chem., Int. Ed.*, 2018, **57**, 1758–1784.
2 T. Pirali, M. Serafini, S. Cargnin and A. A. Genazzani, Applications of deuterium in medicinal chemistry, *J. Med. Chem.*, 2019, **62**, 5276–5297.
3 E. M. Isin, C. S. Elmore, G. N. Nilsson, R. A. Thompson and L. Weidolf, Use of radiolabeled compounds in drug metabolism and pharmacokinetic studies, *Chem. Res. Toxicol.*, 2012, **25**, 532–542.
4 A. Katsnelson, Heavy drugs draw heavy interest from pharma backers, *Nat. Med.*, 2013, **19**, 656.
5 B. Belleau, J. Burba, M. Pindell and J. Reiffenstein, Effect of deuterium substitution in sympathomimetic amines on adrenergic responses, *Science*, 1961, **133**, 102–104.
6 C. Schmidt, First deuterated drug approved, *Nat. Biotechnol.*, 2017, **35**, 493–494.
7 Z. Cao, W. Gao, H. Bao, H. Feng, S. Mei, P. Chen and R. Zhao, VV116 versus nirmatrelvir–ritonavir for oral treatment of Covid-19, *N. Engl. J. Med.*, 2023, **388**, 406–417.
8 V. Jacques, S. Bolze, S. Hallakou-Bozec, A. W. Czarnik, A. S. Divakaruni, P. Fouqueray, A. N. Murphy, L. H. Van der Ploeg and S. DeWitt, Deuterium-stabilized (R)-pioglitazone (PXL065) Is responsible for pioglitazone efficacy in NASH yet exhibits little to no PPARγ activity, *Hepatol. Commun.*, 2021, **5**, 1412–1425.
9 R. M. C. Di Martino, B. D. Maxwell and T. Pirali, Deuterium in drug discovery: progress, opportunities, and challenges, *Nat. Rev. Drug Discovery*, 2023, **22**, 562–584.
10 J. Steverlynck, R. Sitdikov and M. Rueping, The deuterated "magic methyl" group: A guide to site-selective trideuteromethyl incorporation and labeling by using CD_3 reagents, *Chem. – Eur. J.*, 2021, **27**, 11751–11772.
11 C. Teja, S. Kolb, P. Colonna, J. Grover, S. Garcia-Argote, G. K. Lahiri, G. Pieters, D. B. Werz and D. Maiti, Deuteration and Tritiation of Pharmaceuticals by Non-Directed Palladium-Catalyzed C−H Activation in Heavy and Super-Heavy Water, *Angew. Chem., Int. Ed.*, 2024, **63**, e202410162.
12 L. V. Hale and N. K. Szymczak, Stereoretentive deuteration of α-chiral amines with D_2O, *J. Am. Chem. Soc.*, 2016, **138**, 13489–13492.
13 M. Zhang, X. A. Yuan, C. Zhu and J. Xie, Deoxygenative deuteration of carboxylic acids with D_2O, *Angew. Chem., Int. Ed.*, 2019, **58**, 312–316.
14 R. Pony Yu, D. Hesk, N. Rivera, I. Pelczer and P. J. Chirik, *Nature*, 2016, **529**, 195–199.
15 W. Li, J. Rabeah, F. Bourriquen, D. Yang, C. Kreyenschulte, N. Rockstroh, H. Lund, S. Bartling, A.-E. Surkus, K. Junge, A. Brückner, A. Lei and M. Beller, Scalable and selective deuteration of (hetero) arenes, *Nat. Chem.*, 2022, **14**, 334–341.
16 Q. K. Kang, Y. Li, K. Chen, H. Zhu, W. Q. Wu, Y. Lin and H. Shi, Rhodium-catalyzed stereoselective deuteration of benzylic C–H bonds via reversible η6-coordination, *Angew. Chem., Int. Ed.*, 2022, **61**, e202117381.
17 J. Dey, S. Kaltenberger and M. van Gemmeren, Palladium (II)-catalyzed nondirected late-stage $C(sp^2)$−H deuteration of heteroarenes enabled through a multi-substrate screening approach, *Angew. Chemie Int. Ed.*, 2024, **63**, e202404421.
18 S. Kopf, F. Bourriquen, W. Li, H. Neumann, K. Junge and M. Beller, Recent developments for the deuterium and tritium labeling of organic molecules, *Chem. Rev.*, 2022, **122**, 6634–6718.

19 W. Ou, C. Qiu and C. Su, Photo-and electro-catalytic deuteration of feedstock chemicals and pharmaceuticals: A review, *Chinese J. Catal.*, 2022, **43**, 956–970.
20 J. S. Rowbotham, M. A. Ramirez, O. Lenz, H. A. Reeve and K. A. Vincent, Bringing biocatalytic deuteration into the toolbox of asymmetric isotopic labelling techniques, *Nat. Commun.*, 2020, **11**, 1454.
21 T. J. Doyon and A. R. Buller, Site-selective deuteration of amino acids through dual-protein catalysis, *J. Am. Chem. Soc.*, 2022, **138**, 7327–7336.
22 Y. Y. Loh, K. Nagao, A. J. Hoover, D. Hesk, N. R. Rivera, S. L. Colletti, I. W. Dacies and D. W. MacMillan, Photoredox-catalyzed deuteration and tritiation of pharmaceutical compounds, *Science*, 2017, **358**, 1182–1187.
23 C. Liu, Z. Chen, C. Su, X. Zhao, Q. Gao, G.-H. Ning, H. Zhu, W. Tang, K. Leng, W. Fu, B. Tian, X. Peng, J. Li, Q.-H. Xu, W. Zhou and K. P. Loh, Controllable deuteration of halogenated compounds by photocatalytic D_2O splitting, *Nat. Commun.*, 2018, **9**, 80.
24 Z. Zhang, C. Qiu, Y. Xu, Q. Han, J. Tang, K. P. Loh and C. Su, Semiconductor photocatalysis to engineering deuterated N-alkyl pharmaceuticals enabled by synergistic activation of water and alkanols, *Nat. Commun.*, 2020, **11**, 4722.
25 Y. Li, Z. Ye, Y. M. Lin, Y. Liu, Y. Zhang and L. Gong, Organophotocatalytic selective deuterodehalogenation of aryl or alkyl chlorides, *Nat. Commun.*, 2021, **12**, 2894.
26 R. Zhou, L. Ma, X. Yang and J. Cao, Recent advances in visible-light photocatalytic deuteration reactions, *Org. Chem. Front.*, 2021, **8**, 426–444.
27 Q. Shi, M. Xu, R. Chang, D. Ramanathan, B. Peñin, I. Funes-Ardoiz and J. Ye, Visible-light mediated catalytic asymmetric radical deuteration at non-benzylic positions, *Nat. Commun.*, 2022, **13**, 4453.
28 N. Li, J. Li, M. Qin, J. Li, J. Han, C. Zhu, W. Li and J. Xie, Highly selective single and multiple deuteration of unactivated C (sp^3)-H bonds, *Nat. Commun.*, 2022, **13**, 4224.
29 B. Zhang, Z. Zhang, Y. Wang and D. Zhao, Late-stage deuteration and tritiation through bioinspired cooperative hydrogenolysis, *Nat. Synth.*, 2025, **4**, 444–452.
30 J. Xu, J. Fan, Y. Lou, W. Xu, Z. Wang, D. Li, H. Zhou, X. Lin and Q. Wu, Light-driven decarboxylative deuteration enabled by a divergently engineered photodecarboxylase, *Nat. Commun.*, 2021, **12**, 3983.
31 P. L. Norcott, Current electrochemical approaches to selective deuteration, *Chem. Commun.*, 2022, **58**, 2944–2953.
32 D. Wood and S. Lin, Deuterodehalogenation under net reductive or redox-neutral conditions enabled by paired electrolysis, *Angew. Chem., Int. Ed.*, 2023, **62**, e202218858.
33 C. Liu, S. Han, M. Li, X. Chong and B. Zhang, Electrocatalytic deuteration of halides with D_2O as the deuterium source over a copper nanowire arrays cathode, *Angew. Chem. Int. Ed.*, 2020, **59**, 18527–18531.
34 R. Li, Y. Wu, C. Wang, M. He, C. Liu and B. Zhang, One-pot H/D exchange and low-coordinated iron electrocatalyzed deuteration of nitriles in D_2O to α,β-deuterio aryl ethylamines, *Nat. Commun.*, 2022, **13**, 5951.
35 F. Bu, Y. Deng, J. Xu, D. Yang, Y. Li, W. Li and A. Lei, Electrocatalytic reductive deuteration of arenes and heteroarenes, *Nature*, 2024, **634**, 592–599.
36 F. P. Guengerich, Cytochrome P450 and chemical toxicology, *Chem. Res. Toxicol.*, 2008, **21**, 70–83.
37 K. L. Drew and J. Reynisson, The impact of carbon–hydrogen bond dissociation energies on the prediction of the cytochrome P450 mediated major metabolic site of drug-like compounds, *Eur. J. Med. Chem.*, 2012, **56**, 48–55.
38 Z. Zhang and W. Tang, Drug metabolism in drug discovery and development, *Acta Pharm. Sin. B*, 2018, **8**, 721–732.
39 G. Han, G. Li and Y. Sun, Electrocatalytic hydrogenation using palladium membrane reactors, *JACS Au.*, 2024, **4**, 328–343.
40 H. Inoue, T. Abe and C. Iwakura, Successive hydrogenation of styrene at a palladium sheet electrode combined with electrochemical supply of hydrogen, *Chem. Commun.*, 1996, 55–56.
41 R. S. Sherbo, R. S. Delima, V. A. Chiykowski, B. P. MacLeod and C. P. Berlinguette, Complete electron economy by pairing electrolysis with hydrogenation, *Nat. Catal.*, 2018, **1**, 501–507.
42 A. Kurimoto, R. S. Sherbo, Y. Cao, N. W. Loo and C. P. Berlinguette, Electrolytic deuteration of unsaturated bonds without using D_2, *Nat. Catal.*, 2020, **3**, 719–726.
43 G. Han, G. Li and Y. Sun, Electrocatalytic dual hydrogenation of organic substrates with a Faradaic efficiency approaching 200%, *Nat. Catal.*, 2023, **6**, 224–233.
44 A. Kurimoto, S. A. Nasseri, C. Hunt, M. Rooney, D. J. Dvorak, N. E. LeSage, R. P. Jansonius, S. G. Withers and C. P. Berlinguette, Bioelectrocatalysis with a palladium membrane reactor, *Nat. Commun.*, 2023, **14**, 1814.
45 S. R. Marcsisin, X. Jin, T. Bettger, N. McCulley, J. C. Sousa, G. D. Shanks, B. L. Tekwani, R. Sahu, G. A. Reichard, R. J. Sciotti, V. Melendez and B. S. Pybus, CYP450 phenotyping and metabolite identification of quinine by accurate mass UPLC-MS analysis: a possible metabolic link to blackwater fever, *Malar. J.*, 2013, **12**, 1–8.
46 P. Li, C. Guo, S. Wang, D. Ma, T. Feng, Y. Wang and Y. Qiu, Facile and general electrochemical deuteration of unactivated alkyl halides, *Nat. Commun.*, 2022, **13**, 3774.
47 J. R. Widhalm and N. A. Dudareva, familiar ring to it: biosynthesis of plant benzoic acids, *Mol. Plant*, 2015, **8**, 83–97.
48 B. Schweitzer-Chaput, M. A. Horwitz, E. de Pedro Beato and P. Melchiorre, Photochemical generation of radicals from alkyl electrophiles using a nucleophilic organic catalyst, *Nat. Chem.*, 2019, **11**, 129–135.
49 B. V. Varun, K. Vaithegi, S. Yi and S. B. Park, Nature-inspired remodeling of (aza) indoles to meta-aminoaryl nicotinates for late-stage conjugation of vitamin B3 to (hetero) arylamines, *Nat. Commun.*, 2020, **11**, 6308.
50 Z. Y. You, Y. J. Chen, Y. Y. Wang and C. Chen, Synthesis of Deuterium Labeled Standards of 1-Benzylpiperazine, Fenetylline, Nicocodeine and Nicomorphine, *J. Chin. Chem. Soc.*, 2008, **55**, 663–667.

51 C. Sun, M. Zhang, C. Guan, W. Li, Y. Peng and J. Zheng, In vitro and in vivo metabolic activation and hepatotoxicity of chlorzoxazone mediated by CYP3A, *Arch. Toxicol.*, 2024, **98**, 1095–1110.
52 S. Amna, T. Øhlenschlæger, E. A. Sædder, J. V. Sigaard and T. K. Bergmann, Review of clinical pharmacokinetics and pharmacodynamics of clonidine as an adjunct to opioids in palliative care, *Basic Clin. Pharmacol. Toxicol.*, 2024, **134**, 485–497.
53 M. Syed, C. Skonberg and S. H. Hansen, Mitochondrial toxicity of diclofenac and its metabolites via inhibition of oxidative phosphorylation (ATP synthesis) in rat liver mitochondria: Possible role in drug induced liver injury (DILI), *Toxicol. in Vitro*, 2016, **31**, 93–102.
54 D. Ekinci, M. Şentürk and Ö. İ. Küfrevioğlu, Salicylic acid derivatives: synthesis, features and usage as therapeutic tools, *Expert Opin. Ther. Pat.*, 2011, **21**, 1831–1841.
55 P. Ding and Y. Ding, Stories of salicylic acid: a plant defense hormone, *Trends Plant Sci.*, 2020, **25**, 549–565.
56 T. Arif, Salicylic acid as a peeling agent: a comprehensive review. Clin. Cosmet, *Investig. Dermatol.*, 2015, 455–461.
57 G. Ngueta, Caffeine and caffeine metabolites in relation to hypertension in US adults, *Eur. J. Clin. Nutr*, 2020, **74**, 77–86.
58 C. Willson, The clinical toxicology of caffeine: A review and case study, *Toxicol. Rep.*, 2018, **5**, 1140–1152.
59 W. Z. Potter and H. K. Manji, Antidepressants, metabolites, and apparent drug resistance, *Clin. Neuropharmacol.*, 1990, **13**, S45–S53.
60 G. Wozel and C. Blasum, Dapsone in dermatology and beyond, *Arch. Dermatol.*, 2014, **306**, 103–124.
61 Y. A. Siu, M. H. Hao, V. Dixit and W. G. Lai, Celecoxib is a substrate of CYP2D6: Impact on celecoxib metabolism in individuals with CYP2C9* 3 variants, *Drug Metab. Pharmacokinet.*, 2018, **33**, 219–227.
62 K. D. Rainsford, Ibuprofen: pharmacology, efficacy and safety, *Inflammopharmacology*, 2009, **17**, 275–342.
63 M. Nakajima, K. Kobayashi, N. Shimada, S. Tokudome, T. Yamamoto and Y. Kuroiwa, Involvement of CYP1A2 in mexiletine metabolism, *Br. J. Clin. Pharmacol.*, 1998, **46**, 55–62.